doi:10.1016/j.jmb.2006.02.047 J. Mol. Biol. (2006) 358, 1041–1050

JMB

Available online at www.sciencedirect.com

SCIENCE DIRECT®

ELSEVIER

Effects of Ser16 Phosphorylation on the Allosteric Transitions of Phospholamban/Ca^{2+}-ATPase Complex

N. J. Traaseth[1], D. D. Thomas[2] and G. Veglia[1,2]*

[1]*Department of Chemistry University of Minnesota Minneapolis, MN 55455 USA*

[2]*Department of Biochemistry Molecular Biology, and Biophysics, University of Minnesota, Minneapolis, MN 55455, USA*

**Corresponding author*

Phosphorylation by protein kinase A and dephosphorylation by protein phosphatase 1 modulate the inhibitory activity of phospholamban (PLN), the endogenous regulator of the sarco(endo)plasmic reticulum calcium Ca^{2+} ATPase (SERCA). This cyclic mechanism constitutes the driving force for calcium reuptake from the cytoplasm into the myocite lumen, regulating cardiac contractility. PLN undergoes a conformational transition between a relaxed (R) and tense (T) state, an equilibrium perturbed by the addition of SERCA. Here, we show that the single phosphoryl transfer at Ser16 induces a more pronounced conformational switch to the R state in phosphorylated PLN (pPLN). The binding affinity of PLN to SERCA is not affected (K_d values for the transmembrane domains of pPLN and PLN are $\sim$60 μM), supporting the hypothesis that phosphorylation at Ser16 does not dissociate PLN from SERCA. However, the binding surface and dynamics in domain Ib (residues 22–31) change substantially upon phosphorylation. Since PLN can be singly or doubly phosphorylated at Ser16 and Thr17, we propose that these sites remotely control the conformation of domain Ib. These findings constitute a paradigm for how post-translational modifications such as phosphorylation in the cytoplasmic portion of membrane proteins control intramembrane protein–protein interactions.

Keywords: NMR; phospholamban; phosphorylated phospholamban; SERCA; detergent micelles

Introduction

The phospholamban–sarco(endo)plasmic reticulum calcium Ca^{2+} ATPase (PLN/SERCA2a) complex is responsible for maintaining calcium homeostasis in cardiac muscle. In the hypothesized "calcium-induced calcium-release" mechanism, calcium ions are translocated from the lumen into the sarco(endo)plasmic reticulum (SR) *via* the ryanodine receptors for muscle contraction. β-Adrenergic stimulation unleashes cAMP-dependent protein kinase, which phosphorylates PLN at Ser16,[1] a single phosphoryl transfer that is sufficient to reverse inhibition and restore cytosolic calcium to submicromolar concentrations, allowing muscle relaxation.[2]

PLN, a single-pass transmembrane protein, is embedded in SR in a dynamic equilibrium between monomeric active (inhibitory) and pentameric inactive (storage) forms.[3,4] PLN is an L-shaped molecule that comprises three structural domains: a short amphipathic helix (residues 2–16) that is in contact with the surface of the lipid bilayer, a flexible connecting loop (residues 17–21), and a C-terminal helix (residues 22–50) with a highly hydrophobic sequence that is embedded within the membrane.[5,6] NMR and electron paramagnetic resonance (EPR) dynamics analysis further divides PLN into four dynamic domains: the N-terminal cytosolic helix (domain Ia); the connecting loop; and two segments within the C-terminal helix (domain Ib, residues 22–30, part of the cytoplasmic domain, and domain II, residues 31–52, the transmembrane domain).[7,8]

In our previous investigation, using combined NMR and EPR spectroscopies in both detergent micelles and lipid membranes, we demonstrated

Abbreviations used: DPC, dodecylphosphocholine; EPR, electron paramagnetic resonance; PLN, phospholamban; pPLN, phosphorylated PLN; SR, sarco(endo)-plasmic reticulum; SERCA, sarco(endo)plasmic reticulum calcium Ca^{2+} ATPase.

E-mail address of the corresponding author: veglia@chem.umn.edu

that monomeric PLN undergoes a conformational switch, exemplifying an allosteric activation mechanism of membrane protein–protein interaction.[9] Additionally, we found that upon phosphoryl transfer at Se-16, PLN backbone dynamics increase, causing a loss in structural connections between the transmembrane and cytoplasmic domains.[10] Here, we have utilized chemical shift perturbation and differential line broadening[11] to show how these dynamics and conformational changes caused by phosphorylation correlate with changes in structural interactions within the complex, which reverse the functional inhibition of PLN. As in our previous studies, the effects of phosphorylation on the formation of the PLN/SERCA complex were carried out in dodecylphosphocholine (DPC) under fully functional conditions. These studies represent a paradigm for how post-translational modification can influence intramembrane protein–protein interactions.

Results

Direct detection of enzymatic activity of SERCA in the NMR sample

In our previous studies, we reported a loss of ~20% of SERCA activity after 3 h of incubation under NMR conditions.[9] When SERCA's ATP hydrolysis is measured directly using ^{31}P NMR, the enzyme is fully functional and active for many hours under NMR conditions. Upon normalizing the integral of the inorganic phosphate signal to that of DPC in the spectrum, the calcium-dependence of ATPase activity was determined (Figure 1). SERCA activity in 10 mM DPC (above the critical micellar concentration) and at a DPC to SERCA molar ratio of 1667:1 (higher ratio than for the end point of the NMR titrations, 1200:1) shows cooperative ATPase activity (Hill coefficient $n=2.7$), comparing well with results obtained in native, heterologously expressed, and reconstituted membranes.[12–16] More importantly, PLN effectively inhibits SERCA by shifting the calcium curve 0.16($\pm$0.08) pCa units, while phosphorylation fully relieves inhibition. Although this inhibitory shift is less than that observed in reconstituted lipid membranes,[7] and the Hill coefficient ($n=2.7$) is lower, suggesting a decrease in cooperativity, these data are consistent with previous results found in native and reconstituted membranes,[17–19] showing that SERCA remains active and functional under the conditions used for all our NMR experiments, which support both inhibition of SERCA by PLN and relief by either Ca^{2+} or PLN phosphorylation. We measured a V_{max} of ~55 I.U. for control, +PLN, and +pPLN curves in Figure 1. This value is substantially higher than typically observed in membranes, consistent with previous observations that detergent can activate SERCA relative to native membranes.[14]

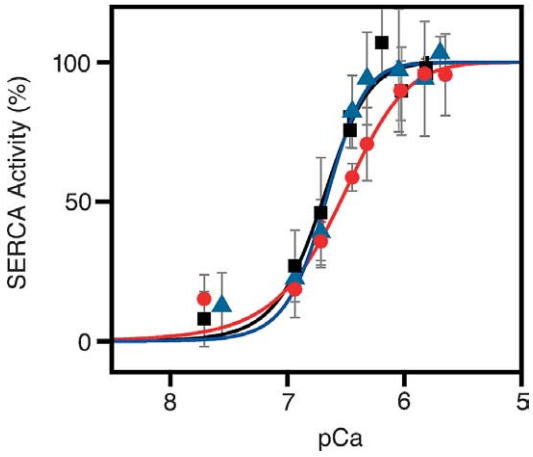

Figure 1. SERCA activity assays using ^{31}P NMR internally referenced to DPC standard. Data are normalized with respect to the V_{max} calculated using the Hill equation (equation (3)). Curves show the effects of PLN (red, circles) and pPLN (blue, triangles) on SERCA activity (rectangles, black). Error bars indicate an average of three trials for SERCA activity alone and two for pPLN and PLN.

Effects of phosphorylation on the allosteric transition of PLN

To monitor the effects of the enzyme addition on the resonances of PLN, we used differential line broadening analysis.[11] This simple approach is ideal for mapping the binding interfaces of protein complexes interacting on an intermediate/slow time-scale with respect to NMR chemical exchange.[11] Addition of SERCA to phosphorylated PLN (pPLN) causes a chemical shift pattern similar to that obtained previously with the unphosphorylated form.[9] According to previously established nomenclature,[9] we apportioned the resonance perturbations into the following groups: (1) resonances that decrease in intensity upon addition of SERCA, but do not disappear; (2) residues that disappear; (3)–(5) residues that undergo slow exchange to one (groups 3 and 4) or two (group 5) additional populations. The chemical exchanging peaks that we detected on the slow NMR time-scale (micro- to milliseconds) were assigned to an intermediate or extended conformation of PLN (R state) that is encoded in PLN dynamics and enhanced by the addition of SERCA. This allosteric activation by SERCA allows the cytoplasmic domain of PLN to be lifted from the bilayer surface from its thermodynamically stable bent (T) state in order to effectively interact with the cytoplasmic domain of SERCA.[9]

The total peak intensities for backbone residues measured in the spectra reflect all of the populations present in solution: R (p_R), T (p_T), and bound (p_{bound}) states:

$$p_{total} = p_R + p_T + p_{bound} \quad (1)$$

Note that, as reported previously, backbone resonances in the bound state are broadened

beyond detection, leading to observable detection of the T and R states only.[9]

The intensities of several resonances of domain Ia for both pPLN and PLN decrease gradually upon addition of SERCA. For instance, the intensity retentions of Glu2, Lys3, Tyr6, and Thr8 gradually decrease, and at a SERCA:pPLN molar ratio of 0.64:1, their signals become undetectably broad (residues plotted in Figure 2(b)). In both pPLN and PLN, the remaining residues of domain Ia (Ser10, Ala11, Ile12, Ala15, Ser16, and Thr17) exhibit slow exchange (micro- to milliseconds) to a second, detectable population (p_R) that we have assigned to the R or extended state (Figure 2(a)).[9]

If we define the intensity of the T state as I_T and the intensity of the R state as I_R, it is possible to monitor the percentage of free PLN in the R state (X_R) throughout the titration of SERCA:

$$X_R = [I_R/(I_R + I_T)] \times 100\% \quad (2)$$

When X_R is plotted against the SERCA:PLN molar ratio, a striking difference between PLN and pPLN emerges (Figure 2(a)). Unlike those of the unphosphorylated form, the pPLN titration curves for slow exchanging residues and those that disappear (Figure 2(a) and (b)) show cooperative behavior, with Hill coefficients of $n = 1.8 \pm 0.6$ and 4.4 ± 0.4, respectively (Figure 3(a)). These data prove that the conformational switch within the cytoplasmic domain from the T to the R state occurs in a cooperative manner, a mechanism less apparent in the absence of phosphorylation. A similar cooperative behavior toward the R state is seen for pPLN residues within the loop (17–21), with such cooperativity not as apparent for unphosphorylated PLN. The loop appears to function in both PLN and pPLN in a manner similar to that of the C-terminal end of domain Ia, demonstrating slow exchange as well as cooperative allosteric behavior for pPLN.

Although a cooperative structural change within the cytoplasmic domain of pPLN toward the R state is apparent from Figure 3(a), the binding of domain II to SERCA of pPLN and PLN is similar (Figures 2(c) and 3(b)), demonstrating that phosphorylation does not cause complete dissociation from SERCA. As with the unphosphorylated form, resonances corresponding to domain II decrease in intensity with increasing amounts of SERCA. To determine the K_d values of domain II, we have repeated the titrations with both PLN and pPLN with smaller increments of SERCA. The resulting binding curves are reported both in Figures 2(c) and 3(b), and were obtained by averaging the intensity retention of residues 28–52 of domain II. Upon fitting the curves using equation (10), we obtained K_d values of 57 μM and 58 μM for pPLN and PLN, respectively (Figure 3(b)). These values agree well with the previously determined dissociation constant of PLN in DPC using EPR spectroscopy (60 μM),[9]

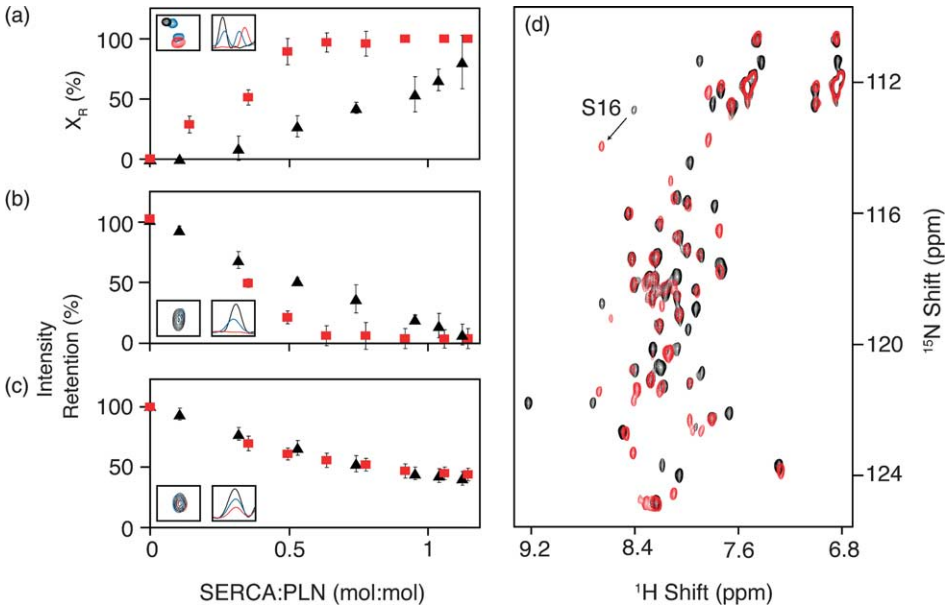

Figure 2. (a) The percentage of free PLN in the R state (X_R, see equation (2)) as a function of the SERCA:PLN molar ratio for phosphorylated (red) and unphosphorylated (black) PLN residues 10–12, 15–17, and 22. An X_R value of 100% indicates that a peak has completely exchanged to the new, extended population (R state). (b) The intensity retention plotted for residues 2, 3, 6, and 8 in pPLN and PLN that disappear with increasing additions of SERCA. (c) The intensity retention for residues in the transmembrane domain (28–52) that decrease, but do not abolish in intensity. All error bars in plots reflect the standard deviation around the average value for residues within a given group. Insets: representative 1D and 2D spectra of the residues undergoing slow exchange (a), abolished intensity (b), and intensity reduction (c). Black, blue, and red spectra in the insets correspond to SERCA:pPLN molar ratios of 0:1, 0.5:1, and 1:1, respectively. (d) The HSQC spectra shown for the presence (red) and the absence (black) of SERCA at a SERCA:pPLN molar ratio of 0.5:1.

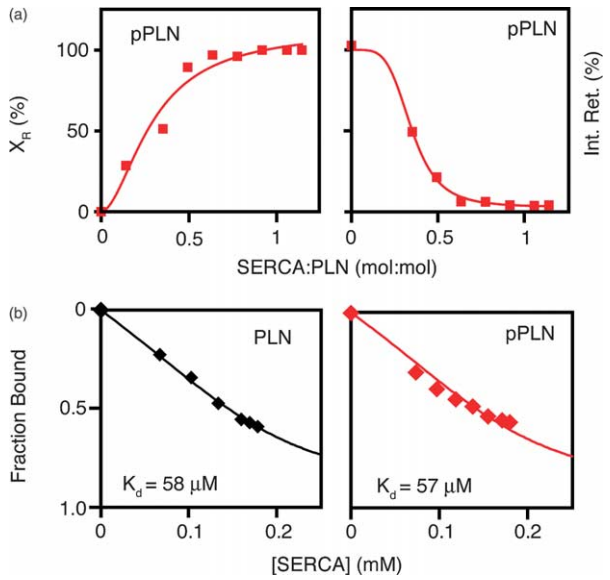

Figure 3. (a) Left: fit of X_R (see equation (2)) as a function of the SERCA:pPLN molar ratio using the Hill equation (data shown in Figure 2(a)). Right: fit of the intensity retention as a function of SERCA:pPLN molar ratio also using the Hill equation (data shown in Figure 2(b)). Fits in (a) show cooperativity of the T to R state transition for pPLN with addition of SERCA with an average Hill coefficient of 3.1 ± 1.3. (b) Determination of dissociation constants (K_d) using intensity retentions of transmembrane domain residues 28–52. Since there is no substantial line broadening (i.e. fast exchange), intensity reduction of these residues can be approximated directly to be an indication of binding (see equation (4)). The K_d values were determined to be 57 μM and 58 μM for pPLN (right) and PLN (left), respectively, from a non-linear regression best fit to equation (10).

and indicate that at low concentrations of calcium (SERCA in the E2 state) domain II has the same affinity for SERCA in both PLN and pPLN.

While the addition of SERCA to pPLN shifts the equilibrium toward the R state at a lower molar ratio of SERCA:pPLN for both domain Ia and Ib (i.e. higher intensity of the R state population), domain Ib, the loop, and residues 15 and 16 of domain Ia also have larger chemical shift differences between the chemically exchanging populations (T and R states; Figure 4). The latter effect suggests that in the phosphorylated form of PLN, the conformational interconversion between the T and the R states occurs on a slower time-scale or that their conformations differ more significantly. Our previous studies show that Ser16 phosphorylation partially unwinds domain Ia and enhances the dynamics of domain Ib in the micro- to millisecond time-scale.[10] From an energetic standpoint, Ser16 phosphorylation lowers the structural activation energy barrier, shifting the dynamic equilibrium toward the R state at a lower molar ratio of SERCA:PLN, while still having the same overall binding affinity for SERCA.

Secondary structural changes in domains Ib and II upon binding to SERCA

Chemical shift perturbations were used as reporters for secondary structural changes in PLN upon binding to SERCA. For folded proteins, upfield or downfield chemical shifts in amide resonances have been correlated with lengths of hydrogen bonds.[20] Specifically, upfield chemical shifts in amide resonances upon binding may be indicative of longer hydrogen bonds, whereas downfield chemical shifts would correspond to shorter hydrogen bonds. Upon the addition of SERCA, the resonances within domain Ib and II of both PLN and pPLN have differential chemical shifts. As Figure 4 (bottom) illustrates, there are three distinct regions of perturbation. The first region (residues 28–42) experiences downfield resonance shifts, the second (residues 43–45) no chemical shifts, and the third region (residues 46–52) upfield shifts. Only ^{1}H $\Delta\delta$ are reported, although a similar trend is seen for ^{15}N frequencies (data not shown). Figure 4 (bottom) shows examples of chemical shift perturbations for three residues, N30, I46, and V49, as representative of peaks undergoing upfield shifts, no shifts, and downfield shifts, respectively. A possible explanation is that upon interaction with SERCA in both pPLN and PLN, residues 28–42 form a tighter helix with stronger hydrogen bonds, residues 43–45 are not substantially altered, and residues 46–52 may have a looser helix with weaker hydrogen bonds. According to Figure 4 (bottom), the structural changes induced by SERCA in the highly hydrophobic residues 34–52 are similar for both pPLN and PLN. These data indicate that domains Ib and II also shift to the R state upon addition of SERCA, which supports the hypothesis of an allosteric switch to the R state, involving a concerted effect involving the entire protein.

Side-chain resonances reveal the role of domain Ib

Unlike the backbone amide resonances, side-chain ^{15}N resonances exhibit a higher degree of local motion and may retain full intensity at the endpoint of our SERCA titrations, making them good indicators of the binding interface.[21] Figure 5 shows the changes in the NH_2 group intensities of the resolved side-chains present in pPLN and PLN. As seen in Figure 5(b), the dotted line represents the intensity retention from the backbone transmembrane domain residues in Figure 2(c), indicating "1-fraction bound" (see equation (4)). Upon addition of SERCA, all of the side-chain ^{15}N resonance intensities (Figure 5(b)) in the unphosphorylated PLN decrease, with the most notable changes occurring for Gln5. The backbone resonances of residues 2–7 (part of domain Ia) gradually disappear upon addition of SERCA, indicating that Gln5 undergoes conformational or intermediate exchange upon addition of SERCA. The remaining

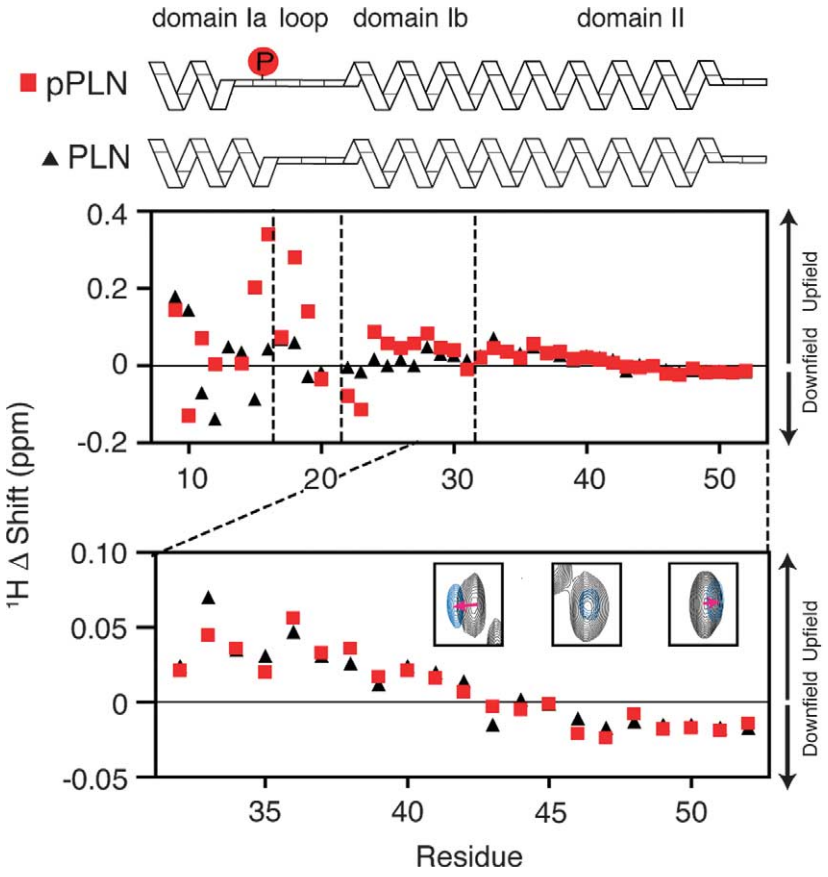

Figure 4. Chemical shift perturbation of backbone resonances. The change in backbone amide proton chemical shifts at a SERCA:PLN molar ratio of 1:1. Top: red squares indicate the perturbation of pPLN, while black triangles indicate those involving PLN. Bottom: same as in the upper plot, but with a closer look at changes involving residues 32–52. The insets in the lower plot are representative spectra of N30 (left), I46 (center), and V49 (right) showing downfield, no, and upfield chemical shift perturbation, respectively.

residues (Gln22, Gln23, Gln26, Gln29, Asn30, and Asn34) are also affected by SERCA addition, which decreases their overall intensities, with Gln22 and Gln23 less affected than the rest of the side-chains. Phosphorylation at Ser16 does not cause any variation in the intensity reduction of Gln5. On the other hand, small but significant differences are observed for Asn27, Asn30, and Asn34, whose

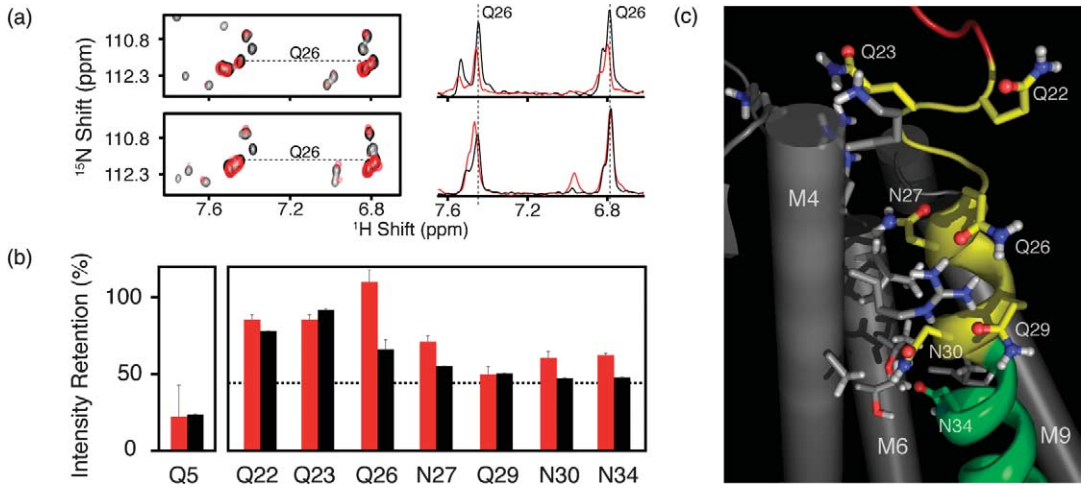

Figure 5. (a) The HSQC spectra for PLN (top) and pPLN (bottom) for the side-chain residues at a pPLN and SERCA:PLN molar ratio of 1:1. The 1D ^{1}H traces (taken from the HSQC spectrum) clearly show the intensity reduction of Q26 for PLN and no intensity reduction for pPLN at a SERCA:PLN molar ratio of 1:1. (b) The intensity retention (%) of side-chain ^{15}N pPLN (red) and PLN (black) resonances at a SERCA:PLN molar ratio of 1:1. The dotted line is the intensity retention (1−fraction of bound) for residues 28–52 (transmembrane domain). A value of 100% indicates no interaction with SERCA (no restriction of motion), whereas a value near the dotted line indicates a strong interaction (restriction of motion). A value below this line would indicate other effects, such as chemical or conformational exchange. Error bars within this Figure reflect the standard deviation from two data sets. (c) The domain Ib side-chains shown on the computational model of the PLN/SERCA complex.[22] Data from (b) indicate that, upon phosphorylation at Ser16, the carboxyl group of the side-chain of Gln26 may no longer form a hydrogen bond with the guanidinium group of Arg324 on SERCA.

intensity retentions vary ~30% from those of the unphosphorylated PLN. The most remarkable difference between PLN and pPLN is observed for Gln26, whose intensity in pPLN is fully retained, indicating that this side-chain is no longer involved in the binding interface. Unfortunately, in the spectrum of pPLN, Gln22 and Gln23 side-chain resonances overlap so it is not possible to distinguish individual resonances. Nonetheless, the sum of their peak intensities remains relatively unperturbed upon addition of SERCA, showing that neither residue is strongly involved in the binding interface with the enzyme.

Mapping the chemical shift perturbations on the structural model of PLN/SERCA complex

Recently, using mutagenesis and cross-linking data, MacLennan and co-workers built a molecular model for the inhibitory interactions between PLN and SERCA.[22] They proposed that during the structural rearrangement of SERCA between the E1 and E2 (high and low calcium-affinity states, respectively) conformations of the enzyme, a docking groove located between transmembrane domains M2 and M9 becomes more accessible to PLN. When modeled in this groove, PLN interacts also with M4 and M6 transmembrane helices, but its domain II does not undergo any substantial structural changes from the initial experimentally determined PLN structure, remaining in a distorted helical conformation after energy minimization. The only changes occurring to PLN upon binding SERCA in the low calcium-affinity state (E2 state) are localized in the C-terminal side of domain II, which unwinds and emerges from the hydrophobic core of the membrane to minimize the free energy of binding. The stability of the helix between residues 42 and 45, and the unwinding of the C terminus (supported also by cysteine mutant cross-linking experiments with Val49 in PLN and Val89 in domain M2 of SERCA[22]) are in agreement with the upfield chemical shifts we observe for residues 46–52, as well as the lack of chemical shift perturbations seen for residues 42–45. Note that domain II binding to SERCA is not affected by phosphorylation (Figure 4, bottom). This is direct evidence that this region binds to SERCA irrespective of the phosphorylation state of PLN. Given the high affinity of PLN for SERCA in lipid membranes,[23] it is possible that the transmembrane domain anchors PLN to SERCA, a finding that would support the hypothesis that PLN is effectively a subunit of SERCA.[23] We found that when titrated with SERCA, sarcolipin, functionally homologous to PLN and sharing ~70% identity (or conserved residues) with PLN, shows the same chemical shift pattern of the corresponding transmembrane domain of PLN.[24] This explains why the sequences of polypeptides corresponding to sarcolipin or the transmembrane domain of PLN are sufficient for enzyme inhibition.[25]

A crucial region identified between SERCA and PLN by cross-linking and modeling is domain Ib.[22,26,27] In fact, one of the structural constraints used in the modeling simulations involves Asn27 of PLN and Leu321 of SERCA.[22] Upon energy minimization, this constraint imposes a substantial structural rearrangement upon domain Ib, with the formation of hydrogen bonds between Asn34 and Thr805 of SERCA. Our NMR binding data show that both of the side-chains of Asn30 and Asn34 are involved in the binding to SERCA, and their decrease in intensity reflects the K_d measured for the transmembrane domain. Phosphorylation slightly affects this region with a total reduction in intensity of about 61% for the side-chain resonances of Asn30 and Asn34, a 14% greater intensity retention than that for unphosphorylated PLN.

A remarkable difference (44% greater intensity retention for pPLN) between the phosphorylated and unphosphorylated states was detected for Gln26 (Figure 5(b)). In the molecular model, the carboxyl group of the side-chain of Gln26 forms a hydrogen bond with the guanidinium group of Arg324.[22] When PLN is unphosphorylated, SERCA addition causes the intensity of the Gln26 side-chains to decrease to 65% intensity retention. In contrast, when PLN is phosphorylated, the intensity of Gln26 is completely retained, suggesting that this side-chain swings away from the binding surface and moves freely, hampering any possible hydrogen bonding.

The chemical shift mapping of domain Ib of PLN shows that these residues undergo downfield shifts upon SERCA binding, suggesting the formation of a more compact structure around this region. Phosphorylation does not reverse the general trend; rather, it significantly affects the chemical shift perturbation of three residues in this region, causing further downfield shifts for residues 24–30 and upfield shifts for Leu31 and Ile33 (Figure 4, top). Indeed, since the bound form of PLN is not visible under our experimental conditions, it is not possible to draw any conclusion about secondary structure changes in this region. Nonetheless, our data strongly suggest that the hydrophobic interactions predicted by the structural model involving domain Ib are disrupted. The importance of this region for the regulatory interactions of PLN has been indicated by functional data.[28] Specifically, alanine-scanning mutagenesis has shown that residues in this region strongly affect the efficacy of PLN inhibition, with N27A and N30A mutants giving rise to super-inhibition of the enzyme.[28]

The results from the molecular modeling of the conformation of the cytoplasmic portion reveal a slight unwinding of this domain, forming a non-ideal helix.[29] Consistent with the molecular modeling, our data show that PLN and pPLN both interact with SERCA. While the residues for both the phosphorylated and unphosphorylated forms show slow exchange between the R and T states

upon binding SERCA, they differ in the population of the R state at a given SERCA:PLN molar ratio (Figures 2 and 4). No complete detachment of PLN is observed for either the cytoplasmic or the transmembrane domain, which is in agreement with the results of several spectroscopic and co-immunoprecipitation studies,[30–32] and recent EPR data.[33] On the basis of these results, we conclude that phosphorylation causes a rearrangement of the interaction surface between SERCA and PLN, with an important role played by the residues located in domain Ib. The most apparent change for side-chain NH_2 groups upon Ser16 phosphorylation occurs at Gln26, which is located in domain Ib of PLN. These changes are attributable mostly to the propagation of dynamics and conformational changes initiated by the phosphoryl transfer. As with both free PLN and pPLN,[8,10] nuclear spin relaxation measurements (T_1, T_2, heteronuclear NOE, and Carr–Purcell–Meiboom–Gill experiments) would provide complete characterization of the dynamic conformational interconversion of PLN in the presence of SERCA. Unfortunately, under our experimental conditions the enzyme becomes inactive after several hours and would lose most of its activity during the course of these lengthy experiments.

The present study in DPC micelles is complementary to the EPR results in lipid bilayers reported by Karim *et al*.[33] As with our previous analysis of the interactions of unphosphorylated PLN,[9] the EPR analysis confirms the existence of the equilibrium between the R and the T states both in the free and bound forms of PLN, and shows that SERCA shifts the equilibrium toward the R state. These equilibria are present in DPC micelles as well as in dioleoylphosphatidylcholine/dioleoylphosphatidylethanolamine (DOPC/DOPE) lipid bilayers. The EPR study also confirms that phosphorylation changes the structural dynamics of the PLN cytoplasmic domain without dissociating PLN from SERCA. The EPR data underscore the importance of these dynamic equilibria for SERCA regulation, showing that hampering the T to R transition prevents the reversal of inhibition by phosphorylation.

Discussion

Molecular signaling in myocytes involves steric, allosteric, and cooperative mechanisms that are modified by protein phosphorylation. These events play a pivotal role in the "beat-to-beat control" of cardiac function. Our laboratory has embarked on the molecular characterization of calcium reuptake into the lumen *via* SERCA and its modulator PLN. Under our NMR conditions, the PLN/SERCA complex is fully functional, showing inhibition by PLN and subsequent relief upon phosphorylation as measured directly using ^{31}P NMR (Figure 1). Although there are obvious issues related to curvature and micellar size, DPC represents a good mimic of native lipid conditions and reproduces functional results obtained by activity assays in lipid membranes.

Previously, phosphorylation at Ser16 of PLN was shown to affect pico- to nanosecond and micro- to millisecond time-scale dynamics throughout PLN, and to disrupt the L-shaped structure of the protein, resulting in an unwinding of cytoplasmic domain residues 14–16.[10] Here, we show that phosphorylation leads to a cooperative allosteric activation of the cytoplasmic domain of pPLN by SERCA, shifting the equilibrium to the extended (R) state of pPLN at a lower SERCA:pPLN molar ratio than that required for unphosphorylated PLN. These new data were anticipated by our previous dynamics studies of pPLN, where it was hypothesized that phosphorylation at Ser16 would lead to an extended and even more disordered state (order-to-disorder transition), reversing SERCA inhibition.[10,34] While the increase in affinity of the cytoplasmic part of PLN toward the R state was an expected result, the role of residues 22–31 (domain Ib) was not predicted. In particular, the analysis of the side-chain data indicates that Gln26, Asn27, Asn30, and Asn34 in PLN associate differently in the PLN/SERCA complex than with pPLN. Since the dissociation constants measured for the residues of domain II of both PLN and pPLN are similar ($\sim$60 μM), we can conclude that phosphorylation does not displace or uncouple domain II of PLN from SERCA; rather, it affects the dynamics of the residues in domain Ib (residues 22–31), leading to a structural rearrangement. Since phosphorylation does not change the electrostatic potential within this region, it is possible that this proposed structural rearrangement is driven by a change in domain Ib dynamics caused directly by phosphorylation at Ser16.

Our results agree well with cross-linking data showing that upon phosphorylation N27C PLN is no longer able to cross-link with L321C of SERCA.[22] This is consistent with our results, which indicate that Asn27 and other residues within domain Ib are less involved in the binding interface with a phosphoryl transfer at Ser16. These results are in good agreement with the mutagenesis studies carried out by MacLennan and co-workers, showing that the Q26A mutant of PLN is a loss-of-function mutant.[28] It is possible that the reduction of the side-chain length and concomitantly the removal of the amino group disrupts the hydrogen bond network and van der Waals interactions between SERCA and domain Ib.

It has been proposed on the basis of mutagenesis data that Lys3 on PLN has a physical interaction with Lys397 and Lys400 within the nucleotide-binding domain of SERCA,[29] with the transmembrane domain partially pulled away from the bilayer. Although this mechanism could explain our chemical shift and side-chain data (Figure 4), further investigation is needed to support this hypothesis.

Taken with our previous studies, these new data complete the overall view of the regulatory

mechanism of PLN, confirming previous spectroscopic investigations. These studies also offer a more detailed map of the residues involved directly in the conformational transitions of PLN during the cyclic regulation of SERCA. The most important conclusion of our investigation is that phosphorylation of PLN, having a predisposition to the R state, facilitates this allosteric transition, modifying the interface between SERCA and PLN rather than detaching the inhibitor. On the basis of the low K_d values obtained in lipid membranes, which were found to be independent of calcium and PLN phosphorylation, Thomas and co-workers proposed that PLN functions under physiological conditions as a subunit of SERCA, which does not detach upon phosphorylation or increasing concentration of Ca^{2+}.[23] The K_d values that we have measured in DPC micelles for the transmembrane residues of both pPLN and PLN support these conclusions and underscore the importance of the cytoplasmic domain as the regulatory domain of PLN.

In summary, we find that phosphorylation at Ser16 does not detach PLN from SERCA, but relays the signal to domain Ib that might function as an intramembrane bridgehead for calcium translocation.[31] In both pPLN and PLN, there is an allosteric conformational switch to a disordered, extended R state for all domains of the protein; however, with phosphorylation this switch is cooperative for the cytoplasmic domain, and can be explained by dynamics and structural differences between pPLN and PLN. We find that phosphorylation influences the dynamics within domain Ib, causing the side-chain of Gln26 to no longer interact with SERCA, and Asn27, Asn30, and Asn34 to have diminished interactions (more mobility). These data firmly link the important structural/functional relationship in biochemistry and structural biology, while opening up the possibility of more advanced spectroscopic studies of the PLN/SERCA complex in detergent micelles and lipid bilayers to further investigate the role of post-translational modifications such as phosphorylation.

Materials and Methods

Protein preparation

Recombinant uniformly ^{15}N labeled unphosphorylated and phosphorylated PLN were prepared as described.[10,15] SERCA2a isoform was purified from rabbit skeletal muscle.[9]

^{31}P NMR activity assays

^{31}P NMR was used to measure the hydrolysis of ATP by SERCA. The components of the final assay mixture consisted of 20 mM Mops (pH 7.0), 6 μM SERCA, 137 μM PLN, 10 mM DPC, 20% glycerol, 1 mM $MgCl_2$, 80 mM ATP, 0.2% (v/v) $C_{12}E_8$, and concentrations of $CaCl_2$ required to reach the concentrations of free Ca^{2+} plotted in Figure 1 (calculated based on the method described by Fabiato and Fabiato[35]). ^{31}P data were collected on a Varian Inova spectrometer operating with a magnetic field strength of 14 T (^{31}P Larmor frequency of 202.349 MHz). Upon addition of nucleotide, eight free induction decays (FIDs) were collected, each consisting of 16 single-pulse transients. Calcium chloride was added incrementally to reach the concentrations of free calcium given in Figure 1. Each calcium curve shown in Figure 1 was acquired on the same SERCA sample in the course of 1 h, and we verified the enzyme's functional integrity by re-measuring maximal SERCA activity after the immediate addition of saturating calcium chloride. The increase in inorganic phosphate was quantified by normalizing to the known amount of DPC in the sample, with the result used subsequently as the amount of ATP hydrolysis. The data were plotted (*V versus* pCa) and fit by the Hill equation:

$$V = V_{max}/[1 + 10^{n(pK_{Ca} - p_{Ca})}] \quad (3)$$

where V is the initial ATPase rate and n is the Hill coefficient. The data were normalized to the maximal rate, V_{max}, which was obtained from the fit, and then replotted to determine the shift in pK_{Ca}. The pPLN/SERCA and PLN/SERCA activity curves in Figure 1 are each an average of two trials, while the control curve is an average of three. Error bars reflect these trials.

NMR sample preparation

Unphosphorylated and phosphorylated, uniformly ^{15}N labeled PLN were prepared in 20 mM PBS (pH 6.0), 300 mM DPC, 10% ^2H_2O to a final concentration of 0.23 mM. SERCA at a concentration of 0.51 mM was added incrementally to the PLN sample as described.[9] To correct for this dilution, and potential pH and salt effects, the same titration experiment was performed with buffer in the absence of SERCA. The components of the SERCA buffer were 20 mM Mops (pH 7.0), 5 mM DPC, 1 mM $CaCl_2$, 1 mM $MgCl_2$, 20% (v/v) glycerol, 0.25 mM DTT, 4 mM ADP. NMR spectra were acquired on a Varian Inova spectrometer operating with a proton Larmor frequency of 600 MHz at 37 °C, using an inverse detection triple-resonance and triple-axis gradient probe. The HSQC pulse program was equipped with pulse field gradients for both coherence selection and sensitivity enhancement.[36] After each addition of SERCA, a ^1H–^{15}N heteronuclear single quantum coherence (HSQC) experiment was done. The ^1H directly detected dimension acquired 1024 points with 16 transients, while the indirectly detected ^{15}N dimension utilized 50 increments. The final matrix size was 1024×1024 real points after zero filling in both dimensions and Fourier transformation. Data were processed using NMRPipe,[37] and viewed using NMRVIEW.[38] Assignments of ambiguous titration spectra were resolved with selective pPLN labels when necessary; PLN titration HSQC spectra have been resolved.[9] The graphics in Figure 5 were prepared using PyMOL†.

K_d measurements by NMR

For measuring the binding constants, we assumed 1:1 binding between SERCA and PLN, and that the intensity reduction ($I_{retention}$) of transmembrane domain residues in Figure 2(c) is related directly to the fraction of PLN bound

† http://pymol.sourceforge.net/

to SERCA (f_b):

$$f_b = 1 - I_{retention} \quad (4)$$

Intensity retention can then be related to a dissociation constant (K_d) through the following derivation, as previously reported using chemical shift:[39]

$$f_b = \frac{[PLN-SERCA]}{[PLN]_f + [PLN-SERCA]} \quad (5)$$

$$K_d = \frac{[PLN]_f[SERCA]_f}{[PLN-SERCA]} \quad (6)$$

$$[SERCA]_t = [SERCA]_f + [PLN-SERCA] \quad (7)$$

$$[PLN]_t = [PLN]_f + [PLN-SERCA] \quad (8)$$

$$K_d = \frac{[SERCA]_t - f_b([PLN]_t - [SERCA]_t) + f_b^2[PLN]_t}{f_b} \quad (9)$$

Taking the negative quadratic solution in equation (9) gives:

$$f_b = \frac{K_d + [SERCA]_t + [PLN]_t - \sqrt{(K_d + [SERCA]_t + [PLN]_t)^2 - 4[SERCA]_t[PLN]_t}}{2[PLN]_t} \quad (10)$$

The dissociation constants were calculated using a non-linear regression best fit of equation (10).

Acknowledgements

This work was supported by National Institute of Health grants GM27906 (to D.D.T.) and HL080081 and GM64742 (to G.V.) and American Heart Association grant 0160465Z. N.J.T. is supported by an American Heart Association Greater Midwest Affiliate Pre-Doctoral fellowship (0515491Z). We thank Jarrod Buffy for helpful discussion; Chikashi Toyoshima and David MacLennan for coordinates of the PLN/SERCA model; Emily Metcalfe, Jamillah Zamoon, and Florentin Nitu for technical assistance. NMR instrumentation at the University of Minnesota High Field NMR Center was funded by the National Science Foundation (BIR-961477) and the University of Minnesota Medical School.

References

1. Simmerman, H. K., Collins, J. H., Theibert, J. L., Wegener, A. D. & Jones, L. R. (1986). Sequence analysis of phospholamban. Identification of phosphorylation sites and two major structural domains. *J. Biol. Chem.* **261**, 13333–13341.
2. Chu, G. & Kranias, E. G. (2002). Functional interplay between dual site phospholambam phosphorylation: insights from genetically altered mouse models. *Basic Res. Cardiol.* **97**, I43–I48.
3. Arkin, I. T., Adams, P. D., Brunger, A. T., Smith, S. O. & Engelman, D. M. (1997). Structural perspectives of phospholamban, a helical transmembrane pentamer. *Annu. Rev. Biophys. Biomol. Struct.* **26**, 157–179.
4. Cornea, R. L., Jones, L. R., Autry, J. M. & Thomas, D. D. (1997). Mutation and phosphorylation change the oligomeric structure of phospholamban in lipid bilayers. *Biochemistry*, **36**, 2960–2967.
5. Mascioni, A., Karim, C., Zamoon, J., Thomas, D. D. & Veglia, G. (2002). Solid-state NMR and rigid body molecular dynamics to determine domain orientations of monomeric phospholamban. *J. Am. Chem. Soc.* **124**, 9392–9393.
6. Zamoon, J., Mascioni, A., Thomas, D. D. & Veglia, G. (2003). NMR solution structure and topological orientation of monomeric phospholamban in dodecylphosphocholine micelles. *Biophys. J.* **85**, 2589–2598.
7. Karim, C. B., Kirby, T. L., Zhang, Z., Nesmelov, Y. & Thomas, D. D. (2004). Phospholamban structural dynamics in lipid bilayers probed by a spin label rigidly coupled to the peptide backbone. *Proc. Natl Acad. Sci. USA*, **101**, 14437–14442.
8. Metcalfe, E. E., Zamoon, J., Thomas, D. D. & Veglia, G. (2004). $^{1}H/^{15}N$ heteronuclear NMR spectroscopy shows four dynamic domains for phospholamban reconstituted in dodecylphosphocholine micelles. *Biophys. J.* **87**, 1–10.
9. Zamoon, J., Nitu, F., Karim, C., Thomas, D. D. & Veglia, G. (2005). Mapping the interaction surface of a membrane protein: unveiling the conformational switch of phospholamban in calcium pump regulation. *Proc. Natl Acad. Sci. USA*, **102**, 4747–4752.
10. Metcalfe, E. E., Traaseth, N. J. & Veglia, G. (2005). Serine 16 phosphorylation induces an order-to-disorder transition in monomeric phospholamban. *Biochemistry*, **44**, 4386–4396.
11. Matsuo, H., Walters, K. J., Teruya, K., Tanaka, T., Gassner, G. T., Lippard, S. J. *et al*. (1999). Identification by NMR spectroscopy of residues at contact surfaces in large, slowly exchanging macromolecular complexes. *J. Am. Chem. Soc.* **121**, 9903–9904.
12. Autry, J. M. & Jones, L. R. (1997). Functional co-expression of the canine cardiac Ca^{2+} pump and phospholamban in *Spodoptera frugiperda* (Sf21) cells reveals new insights on ATPase regulation. *J. Biol. Chem.* **272**, 15872–15880.
13. Fujii, J., Maruyama, K., Tada, M. & MacLennan, D. H. (1990). Co-expression of slow-twitch/cardiac muscle Ca2(+)-ATPase (SERCA2) and phospholamban. *FEBS Letters*, **273**, 232–234.
14. Reddy, L. G., Jones, L. R., Cala, S. E., O'Brian, J. J., Tatulian, S. A. & Stokes, D. L. (1995). Functional reconstitution of recombinant phospholamban with rabbit skeletal Ca(2+)-ATPase. *J. Biol. Chem.* **270**, 9390–9397.
15. Buck, B., Zamoon, J., Kirby, T. L., DeSilva, T. M., Karim, C., Thomas, D. & Veglia, G. (2003). Overexpression, purification, and characterization of recombinant Ca-ATPase regulators for high-resolution solution and solid-state NMR studies. *Protein Expr. Purif.* **30**, 253–261.
16. Voss, J., Jones, L. R. & Thomas, D. D. (1994). The physical mechanism of calcium pump regulation in the heart. *Biophys. J.* **67**, 190–196.
17. Inui, M., Chamberlain, B. K., Saito, A. & Fleischer, S. (1986). The nature of the modulation of Ca2+

transport as studied by reconstitution of cardiac sarcoplasmic reticulum. *J. Biol. Chem.* **261**, 1794–1800.
18. Reddy, L. G., Jones, L. R., Pace, R. C. & Stokes, D. L. (1996). Purified, reconstituted cardiac Ca^{2+}-ATPase is regulated by phospholamban but not by direct phosphorylation with Ca^{2+}/calmodulin-dependent protein kinase. *J. Biol. Chem.* **271**, 14964–14970.
19. Waggoner, J. R., Huffman, J., Griffith, B. N., Jones, L. R. & Mahaney, J. E. (2004). Improved expression and characterization of Ca2+-ATPase and phospholamban in High-Five cells. *Protein Expr. Purif.* **34**, 56–67.
20. Wagner, G., Pardi, A. & Wuthrich, K. (1983). Hydrogen bond length and proton NMR chemical shifts in proteins. *J. Am. Chem. Soc.* **105**, 5948–5949.
21. Kreishman-Deitrick, M., Egile, C., Hoyt, D. W., Ford, J. J., Li, R. & Rosen, M. K. (2003). NMR analysis of methyl groups at 100–500 kDa: model systems and Arp2/3 complex. *Biochemistry*, **42**, 8579–8586.
22. Toyoshima, C., Asahi, M., Sugita, Y., Khanna, R., Tsuda, T. & MacLennan, D. H. (2003). Modeling of the inhibitory interaction of phospholamban with the Ca^{2+} ATPase. *Proc. Natl Acad. Sci. USA*, **100**, 467–472.
23. Mueller, B. K., C, B., Negrashov, I. V., Kutchai, H. & Thomas, D. D. (2004). Direct detection of phospholamban and sarcoplasmic reticulum Ca-ATPase interaction in membranes using fluorescence resonance energy transfer. *Biochemistry*, **43**, 8754–8765.
24. Buffy J., Buck-Koehntop, B. A., Porcelli, F., Traaseth, N. J., Thomas, D. D., Veglia, G., (2006). Defining the intramembrane binding mechanism of sarcolipin to calcium ATPase using solution NMR spectroscopy. *J. Mol. Biol. Accepted*.
25. Karim, C. B., Marquardt, C. G., Stamm, J. D., Barany, G. & Thomas, D. D. (2000). Synthetic null-cysteine phospholamban analogue and the corresponding transmembrane domain inhibit the Ca-ATPase. *Biochemistry*, **39**, 10892–10897.
26. Asahi, M., Kimura, Y., Kurzydlowski, K., Tada, M. & MacLennan, D. H. (1999). Transmembrane helix M6 in sarco(endo)plasmic reticulum Ca(2+)-ATPase forms a functional interaction site with phospholamban. Evidence for physical interactions at other sites. *J. Biol. Chem.* **274**, 32855–32862.
27. Jones, L. R., Cornea, R. L. & Chen, Z. (2002). Close proximity between residue 30 of phospholamban and cysteine 318 of the cardiac Ca2+ pump revealed by intermolecular thiol cross-linking. *J. Biol. Chem.* **277**, 28319–28329.
28. Kimura, Y., Asahi, M., Kurzydlowski, K., Tada, M. & MacLennan, D. H. (1998). Phospholamban domain Ib mutations influence functional interactions with the Ca^{2+}-ATPase isoform of cardiac sarcoplasmic reticulum. *J. Biol. Chem.* **273**, 14238–14241.
29. James, P., Inui, M., Tada, M., Chiesi, M. & Carafoli, E. (1989). Nature and site of phospholamban regulation of the Ca^{2+} pump of sarcoplasmic reticulum. *Nature*, **342**, 90–92.
30. Asahi, M., McKenna, E., Kurzydlowski, K., Tada, M. & MacLennan, D. H. (2000). Physical interactions between phospholamban and sarco(endo)plasmic reticulum Ca^{2+}-ATPases are dissociated by elevated Ca^{2+}, but not by phospholamban phosphorylation, vanadate, or thapsigargin, and are enhanced by ATP. *J. Biol. Chem.* **275**, 15034–15038.
31. Li, J., Bigelow, D. J. & Squier, T. C. (2003). Phosphorylation by cAMP-dependent protein kinase modulates the structural coupling between the transmembrane and cytosolic domains of phospholamban. *Biochemistry*, **42**, 10674–10682.
32. Negash, S., Yao, Q., Sun, H., Li, J., Bigelow, D. J. & Squier, T. C. (2000). Phospholamban remains associated with the Ca^{2+}- and Mg^{2+}-dependent ATPase following phosphorylation by cAMP-dependent protein kinase. *Biochem. J.* **351**, 195–205.
33. Karim C. B., Zhang Z. & Thomas D. D. (2006). Phosphorylation-dependent conformational switch in spin-labeled phospholamban bound to SERCA. *Submitted to J. Mol. Biol*.
34. Paterlini, M. G. & Thomas, D. D. (2005). The alpha-helical propensity of the cytoplasmic domain of phospholamban: a molecular dynamics simulation of the effect of phosphorylation and mutation. *Biophys. J.* **88**, 3243–3251.
35. Fabiato, A. & Fabiato, F. (1979). Calculator programs for computing the composition of the solutions containing multiple metals and ligands used for experiments in skinned muscle cells. *J. Physiol. (Paris)*, **75**, 463–505.
36. Kay, L. E., Keifer, P. & Saarinen, T. (1992). Pure absorption gradient enhanced heteronuclear single quantum correlation spectroscopy with improved sensitivity. *J. Am. Chem. Soc.* **114**, 10663–10665.
37. Delaglio, F., Grzesiek, S., Vuister, G. W., Zhu, G., Pfeifer, J. & Bax, A. (1995). NMRPipe: a multidimensional spectral processing system based on UNIX pipes. *J. Biomol. NMR*, **6**, 277–293.
38. Johnson, B. A. & Blevins, R. A. (1994). A computer program for the visualization and analysis of NMR data. *J. Biomol. NMR*, **4**, 603–614.
39. Johnson, P. E., Tomme, P., Joshi, M. D. & McIntosh, L. P. (1996). Interaction of soluble cellooligosaccharides with the N-terminal cellulose-binding domain of *Cellulomonas fimi* CenC 2. NMR and ultraviolet absorption spectroscopy. *Biochemistry*, **35**, 13895–13906.

Edited by M. F. Summers

(Received 1 December 2005; received in revised form 21 January 2006; accepted 16 February 2006)
Available online 7 March 2006